A BARRIER TO LATERAL DIFFUSION OF PORPHYROPSIN IN *NECTURUS* ROD OUTER SEGMENT DISKS

R. E. DRZYMALA
Department of Radiation Oncology, University of Maryland, Medical School, Baltimore, Maryland 21201

H. L. WEINER
School of Medicine, Yale University, New Haven, Connecticut 06511

C. A. DEARRY
Department of Physiology-Anatomy, University of California, Berkeley, California 94720

P. A. LIEBMAN
Department of Anatomy, University of Pennsylvania, School of Medicine, Philadelphia, Pennsylvania 19104

ABSTRACT Microspectrophotometry was used to study lateral diffusion of the visual pigment, porphyropsin, in the disk membrane in intact mudpuppy (*Necturus maculosus*) rod outer segments (ROS), isolated in frog Ringer's solution. A concentration gradient of unbleached visual pigment was produced on the disks by rapidly photobleaching 40% of the pigment in an area spanning 1/4 or 1/2 of the cell's width. The change in optical density of the cells at 580 nm was then followed with time on either the bleached or unbleached side. The temperature dependence of porphyropsin diffusion yielded a Q_{10} of 2.5 between 10 and 20°C with an activation energy of 12 ± 2 kcal. At completion of pigment diffusion, the center and edge of the disk had, respectively, attained only 90 and 55% of the concentration expected. Computed diffusion coefficients (5.4×10^{-9} cm^2/s) were similar at the center and periphery of the disk immediately after the flash, however, an additional slow component for diffusion was detected at the periphery. A comparison of optical density at 525 nm along the diameter of ROS before and after the flash showed a persistent (20 min) postbleach concentration gradient of unbleached porphyropsin. This suggests that 15% of the prophyropsins may be sequestered into distinct areas on a mudpuppy disk and are not free to diffuse over the whole surface. This argument is supported by the observation that mudpuppy disks are separated into petal-shaped regions by incisures, some of which penetrate nearly to the disk center.

INTRODUCTION

Accumulating evidence points to an important biochemical role for diffusion in membranes of the visual cell. Activity of c-GMP phosphodiesterase of rod outer segments (ROS) appears to be dependent upon collisions with a diffusible photoproduct of visual pigment in suspensions of membrane vesicles derived from the outer segment (Liebman and Pugh, 1979, 1981). When a diffusion controlled enzyme reaction is confined to the plane of the bilayer, an increase in turnover number relative to that in bulk aqueous phase may occur. The reduction from three to two dimensional diffusion increases the frequency of effective collisions between enzyme and substrate (Adam and Delbruck, 1968). This can be of much benefit when a fast reaction is required. Rotational (Brown, 1972; Cone 1972) and translational (Liebman and Entine, 1974; Poo and Cone, 1974) diffusion of visual pigment has been demonstrated in the frog and mudpuppy ROS with diffusion coefficients of 2.25×10^6 rad^2 S^{-1} (Trauble and Sackman, 1973) for rotation in frog membranes and $(3.5–5.5) \times 10^{-9}$ cm^2/s for translation in frog and mudpuppy ROS. Recently, Takezoe and Yu (1981) have found a similar value of $(3.3 \pm 1.2) \times 10^{-9}$ cm^2/s for rhodopsin translation in bovine disk membranes. These membranes are, therefore, quite fluid. At least part of this finding can be attributed to their large content of unsaturated phospholipids (Borggreven, et al., 1970).

The ease with which proteins and lipids can diffuse in a membrane depends upon both the size and shape of the molecules and the strength of interactions between neighboring molecules (viscosity). This is reflected in the rate and the extent of rotational or lateral diffusion. A number of mechanisms that limit diffusion in membranes have been proposed. For example, aggregation of protein molecules may restrict diffusion with increases of size or

changes of shape. Bacteriorhodopsin demonstrates rotational relaxation constants longer than 25 min presumably due to interaction with other bacteriorhodopsin molecules to form a crystalline lattice (Korenstein and Hess, 1978); normal relaxation constants are of the order of microseconds. Similarly, an immobile cytoskeletal network of spectrin and actin molecules exists in the erythrocyte membrane (Lux, 1979). A fraction of erythrocyte band 3 protein exhibits restricted rotational diffusion which is a result of anchorage to the cytoskeleton (Nigg and Cherry, 1980). Other membrane bound proteins can be trapped within the of interstices this network thereby limiting their lateral mobilities to short distances while allowing unrestricted rotational mobility (Steck, 1974; Cherry et al., 1976). With breakage of the connections to cytoskeletal components, blebs of muscle membrane near the end plate region show a 1,000-fold increase in diffusibility of the normally immobile acetylcholine receptor (Tank et al., 1981). Thus, translational mobility may be restricted in certain instances.

With relatively large dimensions (12 μm diam $\times$ 30 μm long) the mudpuppy ROS is an excellent system for the study of visual pigment lateral diffusion using a microspectrophotometer. The organelle has a dense packing of the photolabile integral protein, porphyropsin, in the membranes of disk-shaped saccules that are stacked like poker chips along the length of the rod. The optical density exceeds 0.1 when measured at 525 nm through the diameter of dark-adapted ROS. At this density translational diffusion can be monitored using ARAP (absorption recovery after photobleaching) with signal-to-noise ratios approaching that for FRAP (fluorescence recovery after photobleaching) (Liebman et al., 1981). ARAP, in this instance, has the added advantage of being highly specific for porphyropsin molecules, whereas FRAP is dependent upon the general specificity of binding of a fluorescent probe. Furthermore, the ARAP method introduces no potentially perturbing foreign substances.

In this paper we use ARAP and electron microscopy to probe the structure of mudpuppy ROS disks and examine the translational diffusion of visual pigment therein. The diffusion coefficient, its temperature dependence and the extent of diffusion are determined. Evidence is given here as an amplification of that given to the Biophysical Society (Drzymala et al., 1980) during which we first provided evidence for a barrier to translational diffusion of porphyropsin molecules between the edge and center of *Necturus* ROS disks.

MATERIALS AND METHODS

Preparation of Biological Material for Light Microscopy

Mudpuppies (*Necturus maculosus* were obtained from Connecticut Valley Biological Supply Co., Inc. (Southampton, MA) and could be kept longer than six months in aerated, dechlorinated tap water that was changed weekly. They were fed periodically with small goldfish. Before decapitation under dim red light (λ >650 nm), the animals were dark-adapted overnight. The head was pithed, the eyes dissected, and the retinas removed to a petri dish containing isotonic frog Ringer's solution, phosphate-buffered to pH 7.4. The dissection was performed under infrared light on a dissecting microscope fitted with image converters. The ROS were then shaken from a slice of retina into a drop of frog Ringer's solution on a glass slide. After inclusion of the retina slice to prevent squashing of the isolated outer segments, the suspension of cells was covered with a clean coverslip and sealed with paraffin wax. In some cases retina slices were incubated in 1% glutaraldehyde-Ringer's solution for 10 min at 25°C before mounting to cross link proteins in the ROS.

Preparation of Biological Material for Electron Microscopy

Necturus maculosus were dark-adapted overnight. Eyes were enucleated, hemisected, and the anterior structures removed and discarded. The posterior portion was incubated in a phosphate-buffered Ringer's solution, pH 7.2, for 10 min, then immersed in Ringer's solution containing 1.5% glutaraldehyde for 2 h. Purified 10% glutaraldehyde (Electron Microscopy Sciences, Fort Washington, PA) was analyzed on DW-2 spectrophotometer (American Instrument Co., Inc., Silver Spring, MD). The exact concentration, which varied by up to 30% from the manufacturer's specification, was determined by absorbance at 280 nm (Anderson, 1967). Contamination due to glutaraldehyde polymers, indicated by absorbance at 235 nm, was nondetectable.

Previous investigations (Heller et al., 1971; Nir and Pease, 1973) have shown that ROS cytoplasmic and intradiskal volumes retain osmotic integrity after glutaraldehyde fixation; full permeability is created by osmium tetroxide treatment. Consequently, tonicity of all solutions through postfixation was maintained at 256 mOsm by adjusting the Ringer's solution concentration of NaCl. Other components of the Ringer's solution in millimoles per liter: KCl, 2.0; $CaCl_2$, 0.5; $MgCl_2$, 0.5; Na_2HPO_4, 8.0; KH_2PO_4, 1.7; glucose, 3.3. In calculating tonicity, 1.5% (178.6 mM) glutaraldehyde was taken to exert an osmotic pressure of 172 mOsm (Chambers et al., 1968).

After the initial fixation, tissue was washed in Ringer's solution and postfixed in buffered 1% osmium tetroxide for 2 h. The tissue was again washed in Ringer's solution and dehyrated in a graded alcohol series, each constituent of which contained 0.5% added NaCl to reduce extraction (Millonig, 1966). All operations through dehydration were performed under dim red light at 4°C. Tissue specimens of 1 mm^2 were embedded in a Spurr medium (Polysciences, Warrington, PA) of firm composition. This method provides rapid mixing and infiltration due to its low 60 cP viscosity (Spurr, 1969).

Thin sections (60–100 nm) were cut on an MT2 Porter-Blum ultramicrotome (Ivan Sorvall, Inc., Newtown, CT). Best results were obtained by staining with methanolic 10% uranyl magnesium acetate for 30 min, followed by 0.1% lead citrate for 10 min. In agreement with the findings of Frasca and Parks (1965), this routine led to a reduction of diffuse background staining when compared with results obtained using uranyl acetate. Sections were examined in a JEM 100B electron microscope (Japanese Electron Optics Laboratories, Tokyo, Japan) operated at 80 kV. Careful magnification calibration was performed using a grating replica (Ernest Fullam, Schenectady, NY).

Microspectrophotometry

A single beam microspectrophotometer (MSP) as described by Liebman et al. (1981) was used to measure the optical density orthogonal to the long axis of mudpuppy ROS. The optical arrangement of the MSP is depicted in Fig. 1.

A Jarrell-Ash (1/2 meter) monochromator (Jarrell-Ash Div., Fisher Scientific Co., Waltham, MA) (λ) passed monochromatic light from tungsten source (L) through a rectangular exit aperture (A_1). Its image was focused and demagnified to the dimensions 2.0 μm $\times$ 25 μm at the

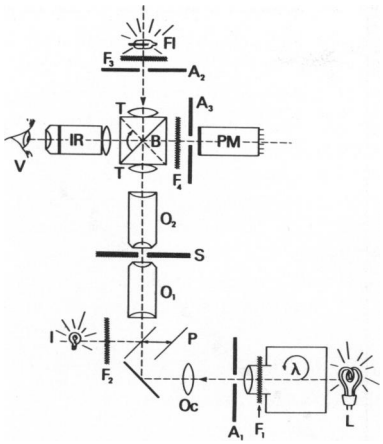

FIGURE 1 Optical design. Light from a tungsten ribbon filament, *L*, is monochromated by λ, linearly polarized by F_1, and formed into a rectangular microbeam by aperature A_1. It then passes through ocular lens, *Oc*, and combines at pellicle beam splitter, *P*, with light from field illuminator, *I*, that has been made infrared by filter, F_2. The two beams are focused upon the stage and specimen, *S*, by objective lens, O_1. Viewer uses objective, O_2, which projects an image to the viewer, *V*, via infrared converter, *IR*, or to photomultiplier, *PM*, depending on the angular position of the beam splitter, *B*. A photoflash from Fl is filtered at F_3, passed through a beam-forming aperture, A_2, and conveyed to the sample via *B* and O_2. The collimator lenses, *T*, assure that A_2 is projected undisplaced by any angular position variation in *B*. F_4 blocks flash wavelengths and A_3 partly prevents flash reflections from reaching *PM*.

specimen plane (S) by a Zeiss Ultrafluar X 32, 0.4 NA lens (O_1) (Carl Zeiss, Inc., Thornwood, NY). Light transmitted by the specimen was collected by a Zeiss ultraviolet condenser (adjusted to 0.4 NA) (O_2) and diverted by the Zeiss beam splitter (B) (Carl Zeiss, Inc.) to an EMI 9558QA photomultiplier (PM) (EMI, Middlesex, England) that could be masked with a filter (F_4). Output of the photomultiplier was converted to log scale with a logarithmic amplifier (4127 KG; Burr-Brown Research Corp., Tucson, AZ) to obtain the optical density (OD). Logarithmic output was simultaneously recorded on an X-Y chart recorder and a PDP-11 computer (Digital Equipment Corp., Marlboro, MA).

Kinetics of Diffusion. The time course of porphyropsin diffusion was followed after photobleaching at 580 nm. The absorption of light at this wavelength by photoproducts is negligible compared with that by porphyropsin. To photobleach the specimen, light from an Acme 242 AR xenon flash gun (Acme Lite Co., Chicago, IL) (Fl) ($t_{1/2} < 10$ ms) was filtered with a Kodak (Wratten No. 48; Eastman Kodak Co., Rochester, NY) color filter (blue) and infrared heat filters (F_3), defined by rectangular aperture (A_2), passed by the beam splitter (B) and focused onto the specimen plane by the objective lens (O_2). The beam splitter was oriented such that it diverted the recording beam to the photomultiplier tube while passing the flash beam to the specimen. A Kodak (Wratten No. 24; Eastman Kodak Co.) (orange) filter (F_4) blocked the flash beam from reaching the photomultiplier tube, thereby reducing the flash artifact and dead time of the electronics. With this arrangement the change in optical density could be monitored within 300 ms of photobleaching of the visual pigment. The flash beam focus was adjusted by observing the image of the aperture reflected from the silvered rule of a stage micrometer mounted on the microscope stage.

A critical factor, alignment of the flash beam with the measuring beam was repeatedly checked during experiments. By sliding a mirror into position at Fl, light from a tungsten bulb was diverted through aperature, A_2, then the microscope to the measure beam aperature, A_1, where the alignment between flash and measure beams could be easily determined and converted to distances in the specimen plane (S). In this manner, the microscope need not be changed (e.g., by beam splitter rotation, specimen removal) from the exact experimental configuration. Assuming a slab model with the boundary conditions and the beam alignment as in Fig. 2 *A* one can solve the diffusion equation and relate the lateral diffusion coefficient for porphyropsin to the rate of OD recovery following photobleaching. The diffusion coefficient, *D*, is given by

$$D = -\frac{L^2}{\pi t_{1/2}} \ln\left(\frac{-0.393}{\cos \pi x/L}\right)$$

(Liebman and Entine, 1974), where *L* is the cell width, *x* is the distance in centimeters from the unbleached edge of the rod, and $t_{1/2}$ is the time to half recovery. For a derivation of this relationship see the Appendix.

Temperature Studies. These were performed with the arrangement described above, however, a Peltier cooler (Cambridge Thermionic, Cambridge, MA) was mounted on the microscope stage. The stage was wrapped with glass wool and aluminum foil to insulate the specimen from ambient room temperature. After waiting an appropriate amount of time for the temperature to equilibrate in the specimen, its temperature was measured with a thermistor in contact with the coverslip. The temperature dependence of porphyropsin diffusion is described by the relationship, $\ln D = \ln(kT/6\pi R\eta_0) - E_a/kT$, where *D* is the diffusion coefficient, *k* is Boltzmann's constant, *T* is absolute temperature, *R* is the radius of the porphyropsin molecule, and E_a is the apparent activation energy. The parameter, η_0, is related to the viscosity (η) through $\eta = \eta_0 \exp(E_a/kT)$. Thus an Arrhenius plot of the diffusion coefficient should yield a straight line for a small range of temperature. The slope gives the activation energy and the intercept gives the thermal energy. For a more detailed mathematical treatment see the Appendix and Tanford (1961).

Optical Density Spectra. Arrangement of the apparatus was similar to that described above, however, the blocking filter, F_4, was removed. OD spectra of ROS were taken between 350 and 650 nm and computer stored. A previously recorded baseline could then be subtracted. Spectra before and after completely photobleaching the cell were obtained to distinguish between OD due to visual pigment absorption and that due to scattering.

Bleach Profiles. The optical density at 525 nm, the absorption maximum for porphyropsin, was measured for seven positions along the diameter of glutaraldehyde-fixed or glutaraldehyde-free ROS as shown in Fig. 6 *A*. The ROS were then photobleached (40%) with a single flash for the three beam configurations: at the edge, in the center, and covering one half of the diameter. After the photoproducts had decayed and diffusion was complete (usually 5 min for glutaraldehyde free cells) the OD at the seven positions were again measured.

Optical density spectra were obtained for each of the seven profile positions to distinguish between absorption and scattering. The measure beam's path length (*L*) through the cell was calculated for each position using Beer's law and by assuming a homogeneous 3 mM porphyropsin concentration before photobleaching and a molar absorption coefficient (ϵ_m) of 43,000 at 525 nm. The profile data could then be simply reduced to changes in visual pigment concentration with the following equations $[OD_A - OD_B]_{meas} = [OD_P]_A + [OD_{scatt}]_A - [OD_P]_B - [OD_{scatt}]_B$. Experimentally, $[OD_{scatt}]_A = [OD_{scatt}]_B$, then $[OD_A - OD_B]_{meas} = [OD_P]_A - [OD_P]_B$ and $[OD_A - OD_B]_{meas}/\epsilon_m L = \Delta C_P$, where the *OD*'s are optical densities at 525 nm, *L* is the path length, ϵ_m is the molar absorption coefficient, and ΔC_P is the change in porphyropsin concentration. The subscripts A, B, P, scatt, and meas represent after photobleaching, before photobleaching, porphyropsin, scattering, and measured, respectively.

RESULTS

By varying the configuration of the ROS, measure and flash beams, we demonstrate in Figs. 2 and 3 that the change in optical density at 580 nm, following an asymmetric photobleach of the ROS, is a consequence of lateral diffusion of porphyropsin in the plane of disk membranes. This conclusion is based on the following observations. (*a*) Controls show no evidence of photoproduct contributing significantly to the optical density changes at 580 nm (Fig. 2 *B*). (*b*) The measuring beam intensity is sufficiently low photobleaching an insignificant amount of pigment during the time course of the experiment (Fig. 2 *D*). (*c*) Traces *A* and *C* (Fig. 2) are mirror images of each other implying that unbleached visual pigment diffuses into the bleached area with accompanying loss from the unbleached side. (*d*) The time course of OD loss is matched by the OD gain for the mirror image configuration (Fig. 3).

From the half-time to recovery (15 s) presented in Fig. 2 *A*, we calculate a translational diffusion coefficient of 5.4 $\times$ 10^{-9} cm^2/s at 22°C. Although this agrees well with the previously published results of this laboratory (D = 5.5 $\times$ 10^{-9} cm^2/s; see Liebman and Entine, 1974), it is 38% larger than the value (D = 3.9 $\times$ 10^{-9} cm^2/s) obtained by Poo and Cone (1974) for mudpuppy ROS. We find that the temperature dependence for lateral diffusion (Q_{10} = 2.5; 10–20°C) exhibited by Fig. 4 *A* is within experimental error of that found by Poo and Cone (1974) (Q_{10} = 3.1 ± 1.4; 17–24°C). An Arrhenius plot of our data (Fig. 4 *B*), however, yields an apparent activation energy of 12 ± 2 kcal/mol as compared with their 21 kcal/mol.

In spite of our meticulous care in handling the ROS and in maintaining a sharp focus of the flash and precise beam alignments, the recovered optical density was consistently

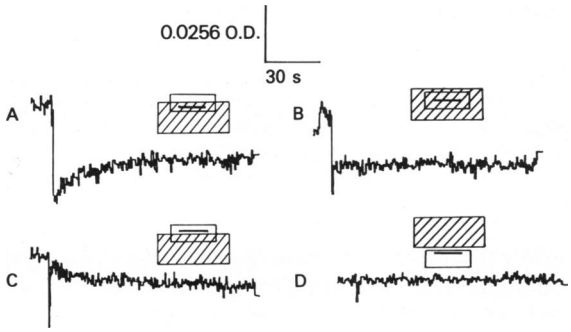

FIGURE 2 Changes of mudpuppy ROS optical density at 580 nm in response to a flash, which, through a 0.4 NA objective, bleaches 40% of the visual pigment within the area illuminated. Beam configurations for the traces are shown above each trace. The open rectangle, the small, solid rectangle, and the large hatched area represent the relative positions of the ROS, the measure beam, and the flash beam, respectively. The flash occurs 15 s after the beginning of each trace. Trace *A* show the OD change with time due to porphyropsin diffusing into the bleached side of the cell, while *C* shows the OD change due to visual pigment movement out of the unbleached into the bleached side. Trace *B* proves that photoproducts do not contribute to the measurement, and *D* demonstrates sharp focus of the flash and insignificant bleach by the measure beam.

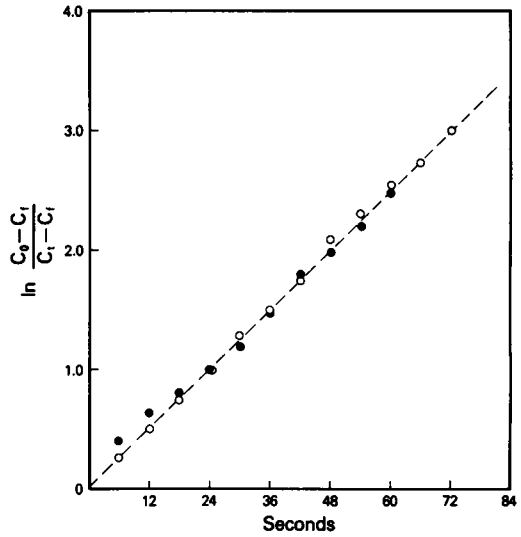

FIGURE 3 A plot against time for normalized porphyropsin gained while using configuration *A* (○) and that lost using configuration *C* (●) of Fig. 2. C_0 and C_f are the initial and final concentrations, respectively. Superimposition shows that they have the same time course and suggests that they result from the same process.

less than expected. For example, a 50% recovery of OD is expected on the bleached side for the configuration in which the flash bisects the cell. Only 35% of the optical density recovered (Fig. 5, trace 1), implying that 30% of the porphyropsin molecules are not free to diffuse into the bleached side. This phenomenon is emphasized in trace 2 of Fig. 5 in which there is much less than the 70–80% return expected for the beam configuration (40% bleach along 1/4 the diameter). A comparison of traces 1 and 2, Fig. 5, suggests that the periphery of the disk has a smaller fraction of diffusible molecules than does the center. This implies a mechanism or structure that preferentially retards only a fraction of the diffusible porphyropsin molecules at the edge. A failure to allow the system to reach equilibrium after photobleaching does not explain the small returns, since following the diffusion for up to 20 min shows no apparent change from that at 2 min.

Although the intensity was reduced so that a flash provided only a 40% bleach, significant blume or scattering might occur at the edge of the flash beam. Also, using convergent optics (NA = 0.4) does not provide a straight, bleach edgethrough the cross-section of the ROS. Either occurrence may allow for a greater bleach of surrounding pigment than the configuration predicts. To determine the degree that convergent optics would affect our results, ray tracing was performed and the total area of the cell illuminated by the flash was calculated. We were not able to account for the reduced recovery by this method. The remaining factor, blume effect, could not be determined easily so a series of optical density profiles were obtained for glutaraldehyde fixed and glutaraldehyde-free cells.

The concentration of visual pigment was compared at seven positions along the diameter of each cell before and

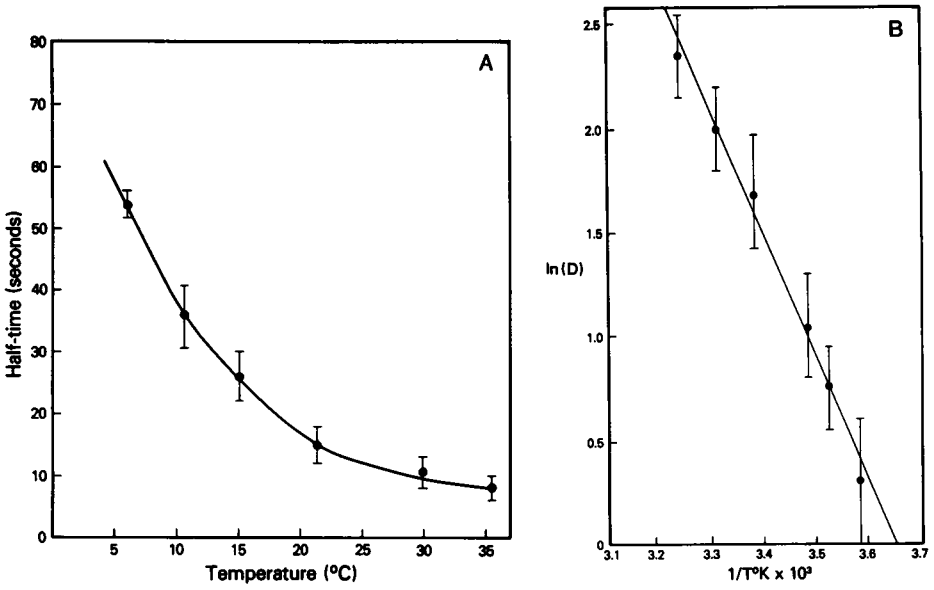

FIGURE 4 The halftime to completion of lateral diffusion (*A*) and the calculated diffusion coefficient (*B*) are plotted as a function of temperature. Error bars represent ± SD resulting from a sampling of 5 cells for each point. The activation energy calculated from the slope of the Arrhenius plot (*B*) is 12 ± 2 kcal/mol.

after photobleaching (see Fig. 6 *A*). Compiled averages of the change in concentration due to photobleach is plotted against position in Fig. 6 *B*, *C*, *D* for 3 beam/cell configurations. A striking concentration gradient of porphyropsin persists in glutaraldehyde-free cells for each of the beam/cell configurations. Comparisons with fixed cells show that roughly 15% (see Discussion) of the porphyropsin does not diffuse between the edge and the center of the disk. Good mixing does occur among porphyropsins within the center of the disk, however.

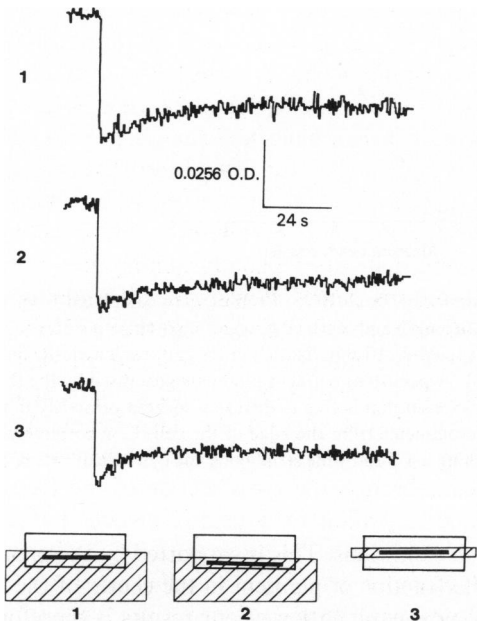

FIGURE 5 Diffusion of visual pigment into the measure beam after a 40% bleach for three beam configurations. The bleach occurs at 12 s after the start of the trace. The OD returns are (*1*) 90%, (*2*) 55%, and (*3*) 60% of that expected, indicating limited diffusion between the edge and center of the disks. Initial diffusion halftimes are (*1*) 15.6 s, (*2*) 15.6 s, and (*3*) 7.2 s, which for configuration *1* corresponds to a diffusion coefficient of 5.4 ± 1.2 × 10^{-9} cm^2/s. Trace *2* shows a slow OD gain at long times not observable with the other beam configurations.

Electron Microscopy

To provide a morphological basis for a population of trapped visual pigment molecules, we include electron micrographs of cross and longitudinal sections of the mudpuppy rod outer segments (Figs. 7 and 8). Our micrographs are similar to those of frog ROS (Cohen, 1972) showing very deep incisures converging from the edge toward the center of *Necturus* disks to form the lobes. The incisures appear to pinch and completely isolate a few of the lobes.

DISCUSSION

We have shown by absorption recovery after photobleaching and by absorption profile measurements that a substantial amount of porphyropsin is unable to diffuse freely about the disks of mudpuppy ROS. These immobile visual pigment molecules seem to reside near the periphery of the disk with irregular radial symmetry. This is not the first time data have been presented for immobile visual pigments. Goldsmith and Wehner (1977) have shown that both rotational and translational-diffusion of visual pigment is absent in the rhabdomeric photoreceptor.

If the nondiffusing porphyropsin molecules of *Necturus* rods occupy the area of the disk swept by the outer 1.6 μm of its 5 μm radius, as indicated by the bleach profiles, they would occupy 50% of the disk area. If there is a homoge-

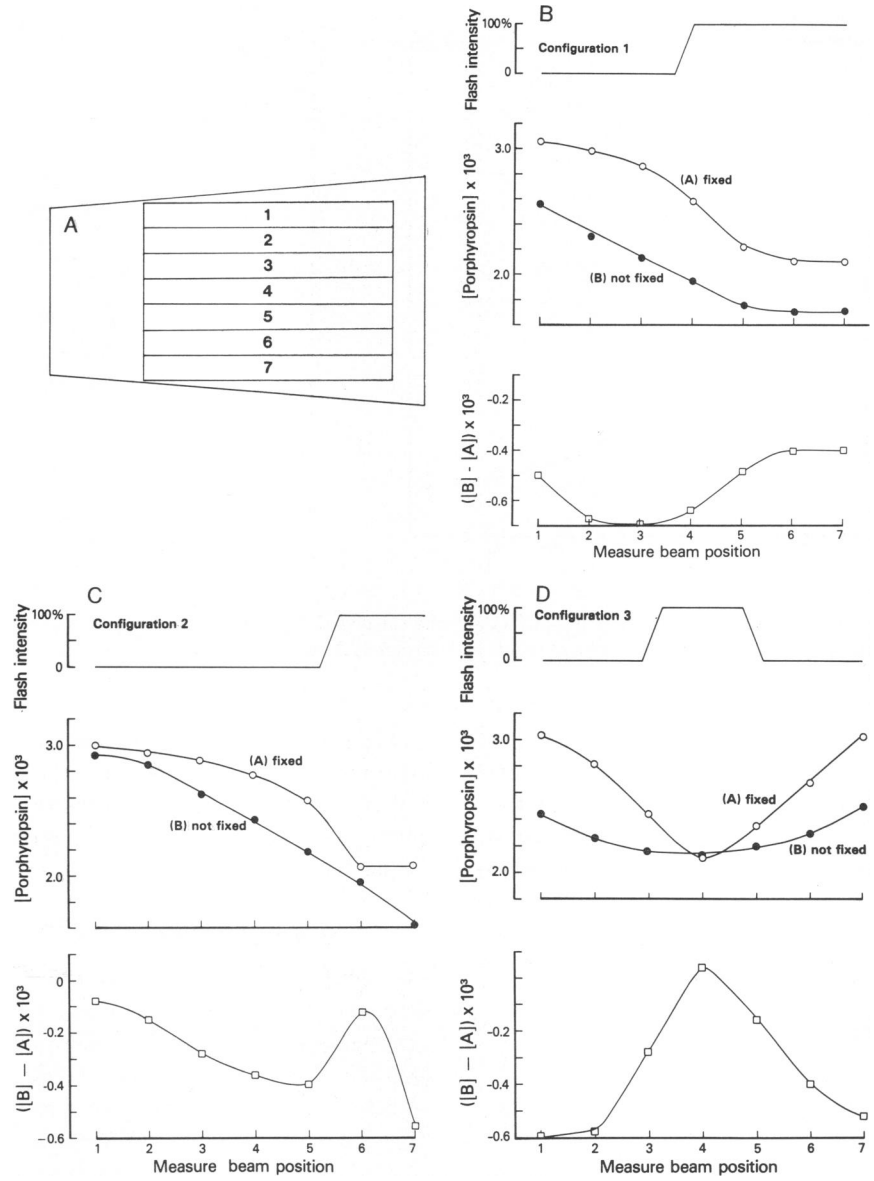

FIGURE 6 (*A*) OD_{525} was measured at the indicated seven positions along the diameter of each ROS. Profiles were calculated from the optical density difference due to bleaching of the cell. The results are corrected for path length and scattering to give pigment concentration at each position. (*B*) Profiles of pigment concentration in ROS after a bleach that bisects fixed (○, 10-min fixation in 1% glutaraldehyde-Ringer's solution) or unfixed cells (●). Profiles of fixed and unfixed cells 20 min after bleach show persistent pigment gradients generated by the flash beam. A profile difference between fixed and unfixed cells (□) indicates that porphyropsin that is free to diffuse is located primarily in the center of disks. (*C*) The profile after bleaching only to a distance, which is 1/4 the diameter from the edge of the cell. Few porphyropsin molecules are available to diffuse into the bleached area. (*D*) The profile after bleaching a 1.5-μm wide strip along the cylindrical axis of the ROS. A more homogeneous distribution results for this configuration after diffusion.

neous distribution of porphyropsins on the disk, 50% of the porphyrosin molecules reside in this area. We know from diffusion recovery at the edge of the disk that 30% of the pigment molecules do not diffuse there. This implies 15% of the total number of porphyropsin molecules are isolated from the center of the disk.

Although paramagnetic resonance spectroscopy has shown that rhodopsin from bovine retina can aggregate with prolonged illumination (30 min at 37°C) or delipidation (Baroin et al., 1979), we did not expose our rods to such harsh conditions. This is supported by the presence of the mobile fraction of pigment in the center of the disk. A morphological explanation of our results is therefore warranted. The incisures found in mudpuppy disks seem likely to play a role in limiting porphyropsin diffusing about the disk surface. Measurements of heat diffusion in metal analogues of mudpuppy disks (Poo and Cone, 1974) predict that the incisures must be very deep to substantially affect the rate of porphyropsin diffusion, and that they must completely pinch off the lobe to limit the number of

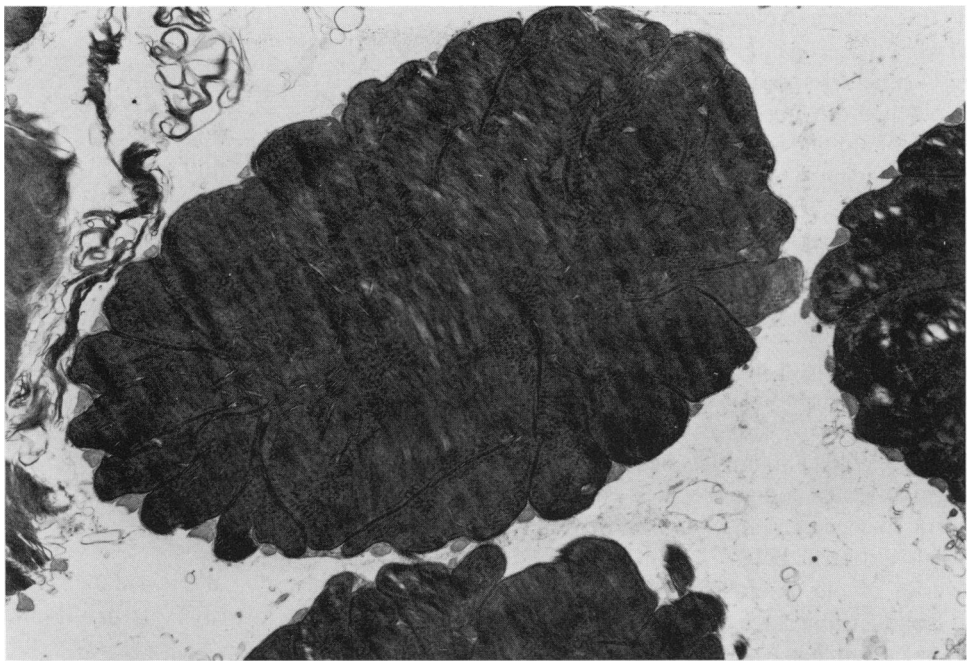

FIGURE 7 An electron micrograph of a ROS cross section with a magnification of 9,459. The lobular structures are outlined by deep incisures that nearly isolate the lobes.

molecules diffusing between the edge and center of the disk. The incisures have been proposed to slow the diffusion of visual pigment in frog ROS (Poo and Cone, 1974; Wey and Cone, 1981). Our electron micrographs of mudpuppy ROS show that the incisures are indeed deep in these cells. A few lobes appear to be isolated by the incisures. Deep incisures would be expected to slow the diffusion or restrict it to a defined area. Our data comparing diffusion of mobile visual pigment in the center with that at the edge of the disk gives little difference for the calculated diffusion coefficient in these regions immediately after the bleach, however, there is a hint of a slow phase at long times in

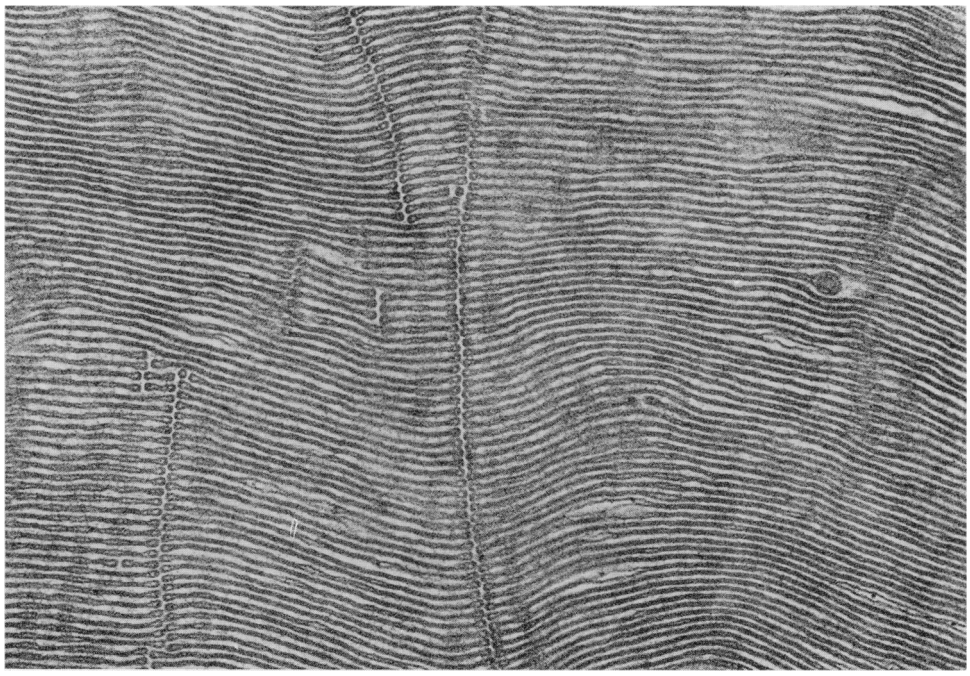

FIGURE 8 An electron micrograph of a ROS longitudinal section with a magnification of 72,900. The hairpin loops occur at the periphery of the disks and the incisures. The incisures are in register for a limited number of disks along the length of the ROS.

some of the kinetic traces. Two explanations reconcile our diffusion data with what we see in our micrographs (*a*) that we have a mixture of pinched and connected lobes or (*b*) that we only have pinched off lobes and those appearing connected are artifacts of oblique sectioning, since sectioning, which is not perpendicular to the rod axis, will result in micrographs of cross sections that do not show the entire length of the incisures. For case *b* above, we must account for the diffusion that we can detect occurring at the edge of the disk. Longitudinal sections show that the incisures are in register for only a short distance. What we see with our microbeam running the length of a ROS results from a population of disks having their lobes at different angles of rotation about the rod axis. Diffusion of visual pigment within lobes that span bleached and unbleached areas may explain our observed diffusion along the disk edge and fewer mobile pigment molecules than would be expected for a confluent disk should be detected. This may account for the poor recoveries of our photobleach experiments while still allowing fast diffusion rates.

Another membrane protein has been shown not to freely diffuse about the disk surface. Papermaster et al. (1978) have identified a 290,000 dalton intrinsic protein glued to the incisures of frog disk. Analogous proteins in the rod outer segment have been found for different species: human, rabbit, and cow (Converse, 1979). The immobility of rod proteins points to the presence of a diffusion barrier associated with the incisures and the edge of the disk. A good candidate for this barrier is a highly viscous mucopolysaccharide gel which exists in high concentration (Drzymala et al., 1982) within the disk near its periphery (Röhlich, 1976; Corless, 1980). This substance may restrict the mobility of porphyropsin.

Whether limited diffusion of porphyropsin plays a central role in visual function is a matter for speculation. We have not shown whether this phenomenon is common to all species. Limited diffusion either by incisures or a barrier substance might reduce the activation of phosphodiesterase (PDE). This may be of benefit near the periphery of the disk, adjacent to the plasma membrane of the rod, where an active PDE is expected to exert a greater influence on the plasma membrane potential than one in the center. Besides affecting the diffusion, lobulation may partition Ca^{++} stores within the disk. This would reduce the number of Ca^{++} released per photon, thereby sparing stores for response to subsequent photons impinging upon other compartments. The above control mechanisms may be necessary in rod outer segments of such large size.

APPENDIX

Mathematical Modeling and Diffusion Theory

Dependence of the Diffusion Coefficient on Bounding Conditions. The diffusion equation used is for the system pictured in Fig. 9. The rod is assumed to have a square cross

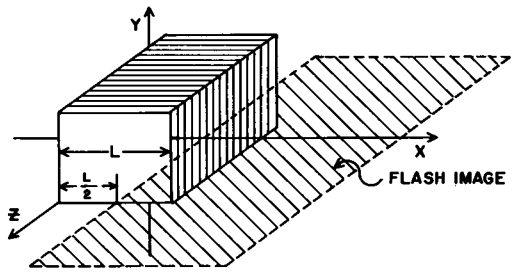

FIGURE 9 The rod outer segment is depicted as a rectangular solid of width L. The flash (hatched area) bisects the ROS at $L/2$ along the x-axis

section of width L, and the disks are approximated as square plates. Since the disks are distinct, no diffusion can occur in the Z-direction. Further, the flash is assumed to cause a uniform bleach in the Y-direction, thus, no concentration gradient exists in the Y-direction. The diffusion will therefore take place in the X-direction only, and the diffusion equation is

$$\frac{d^2C}{dx^2} = \frac{1}{D}\frac{dC}{dt}. \tag{A1}$$

The general solution is described by the series,

$$C(x, t) = \sum_{n-0}^{n-\infty}[A_n\cos(q_n x) + B_n \sin(q_n x)] \exp(-q_n^2 Dt). \tag{A2}$$

The constants A_n, B_n, and q_n must be evaluated on the basis of the initial and boundary conditions to obtain the particular solution.

$$\frac{dC}{dx} = 0 \text{ at } x = 0,$$

$$0 = \sum_{n-0}^{n-\infty}[-A_n q_n \sin(0) + B_n q_n \cos(0)] \exp(-q_n^2 Dt),$$

therefore, $B_n = 0$.

$$\frac{dC}{dx} = 0 \text{ at } x = L,$$

$$0 = \sum_{n-0}^{n-\infty}[-A_n q_n \sin(q_n L)] \exp(-q_n D^2 t),$$

therefore, $q_n = n\pi/L$.

The boundary conditions have simplified the solution to a series of cosines

$$C(x, t) = \sum_{n-0}^{n-\infty} A_n \cos\left(\frac{n\pi x}{L}\right) \exp\left(-\frac{n^2\pi^2 Dt}{L^2}\right). \tag{A3}$$

The constants, A_n, must be evaluated from the initial conditions. At $t = 0$ the solution is a Fourier cosine series that describes the initial concentration distribution across the rod. The distribution is obtained experimentally by an instantaneous bleach causing a drop in porphyropsin concentration, C_B, across part of the rod. The maximum diffusional change will occur when the flash bisects the rod, therefore, the condition desired is

$$C(x, 0) = C_0 \quad \text{for } 0 < x < L/2$$
$$= C_0 - C_B \quad \text{for } L/2 < x < L.$$

The Fourier cosine series must give the periodic function illustrated above. In the region from $x = 0$ to $x = L$, this function describes the

bleach profile. The A_n's are Fourier coefficients and can be calculated from

$$A_n = \frac{2}{L}\int_{x-0}^{x-L} C(x,0)\cos\left(\frac{n\,x}{L}\right)dx. \quad \text{(A4)}$$

The results are $A_0 = C_0 - C_B/2$, $A_n = 0$ for even n, and $A_n = (-1)^{n-1}\,2C_B/n\pi$ for odd n. The complete solution satisfying the experimental boundary, and initial conditions is

$$C(x,t) = C_0 - \frac{C_B}{2} + \sum_{n-1}^{\infty}\frac{(-1)^{n-1}2C_B}{n\pi}\cos\left(\frac{n\pi x}{L}\right)\exp\left(-\frac{n^2\pi^2Dt}{L^2}\right), \quad \text{(A5)}$$

where n is an odd integer. This series solution converges very rapidly. The time dependence is contained solely in the exponential, which increases as n^2. Since only odd n terms appear, the second term ($n = 3$) decays nine times as fast as the first term ($n = 1$), and its effect is only seen in the first few seconds following the bleach. The later terms ($n >$ or $= 5$) are negligible.

The second term can be maximized by choosing $x = 0.6(L)$. Under this condition, the pre-exponential factor of the second term is larger than the first and the sum is necessary to specify the diffusional recovery. For $x = 0.8(L)$, the pre-exponential of the second term is small and the first term alone specifies the return. Experimentally, the concentration of porphyropsin at a given x value is measured by means of the measuring beam of the microspectrophotometer. The width of this beam is not negligible compared with the cell width, thus what is measured is the average of the solution across the width of the measure beam. The beam is of width bw, and is centered on x. What is measured is an average concentration, $\bar{C}(x,t)$,

$$\bar{C}(x,t) = \frac{1}{bw}\int_{x-1/2bw}^{x+1/2bw} C(x,t)\,dx. \quad \text{(A6)}$$

Integration over the $n = 0$ and 1 terms only gives

$$\bar{C}(x,t) = C_0 - \frac{C_B}{2} + \left(\frac{2L}{bw\pi}\right)\sin\left(\frac{bw\pi}{2L}\right)\frac{2C_B}{\pi}\cos\left(\frac{\pi x}{L}\right)\exp\left(-\frac{\pi^2Dt}{L^2}\right). \quad \text{(A7)}$$

This differs from the unaveraged solution by the correction factor $[2L/bw\pi]\sin[bw\pi/2L]$, and is the formal solution that describes diffusion under experimental conditions. The correction factor, however, is close to 1 and the unaveraged single term solution is adequate.

At $t_{1/2}$ after a bleach, the diffusional recovery is half complete and $C = C_0 - (3\,C_B/4)$. Substituting and solving for D one obtains

$$D = -\frac{L^2}{\pi^2 t_{1/2}}\ln\left(\frac{-\frac{\pi}{8}}{\cos\frac{\pi x}{L}}\right). \quad \text{(A8)}$$

L is the cell width in centimeters, and x is the distance in centimeters from the center of the measure beam to the unbleached edge of the cell. The diffusion coefficient, D, will then be expressed in cm^2/s. This was the solution used by Liebman and Entine (1974).

Dependence of Diffusion Coefficient on Temperature. The hole theory of diffusion (Frenkel, 1955; Jost, 1952) provides the theoretical context for the temperature dependence of the process, as well as its activation energy. Diffusion is depicted as a series of jumps of the diffusing particles (porphyropsin molecules) into holes between molecules of the medium (membrane lipid). The activation energy represents the energy necessary to form the hole. The principal effect of temperature on the diffusion is through the rate at which holes can form in the medium.

The mobility, u, of a particle depends on its shape as well as the resistance of the medium to movement through it. This latter quantity is the viscosity, η, of the medium. For spherical particles of radius R, Stokes derived the relationship (Tanford, 1961),

$$u = \frac{1}{6\pi\eta R}. \quad \text{(A9)}$$

The relationship between the diffusion coefficient and the mobility, first deduced by Einstein is

$$D = ukT. \quad \text{(A10)}$$

This can be derived from a pure statisical mechanics approach, as well as from thermodynamics. The latter approach compares Fick's first law with the general phenomenological equation for flow in response to a gradient in potential energy. In the case of diffusion, the gradient is in the chemical potential (Tanford, 1961). Substitution of the equation

$$\eta = \eta_0\exp(E_a/kT), \quad \text{(A11)}$$

into Eq. A9 for η and rearrangement gives

$$u = \frac{1}{6\pi R\eta_0}\exp(-E_a/kT). \quad \text{(A12)}$$

The final form of the equation then can be obtained by substituting the right side of Eq. A12 for u in Eq. A10 and taking the logarithm of both sides to arrive at

$$\ln D = \ln\frac{kT}{6\pi R\eta_0} - E_a/k\left(\frac{1}{T}\right). \quad \text{(A13)}$$

We are grateful to Barbara Dearry and Susan Barth for their help in preparation of this manuscript. This work was supported in part by grants EY0012, EY001583, and EY07035 from the National Eye Institute.

Received for publication 19 May 1983 and in final form 7 October 1983.

REFERENCES

Adam, G., and M. Delbruck. 1968. Reduction of dimensionality in biological diffusion processes. *In* Structural Chemistry and Molecular Biology. Alexander Rich and Norman Davidson, editors. W. H. Freeman and Co., San Francisco. 198–215.

Anderson, P. 1967. Purification and quantitation of glutaraldehyde and its effect on several enzyme activities in skeletal muscles. *J. Histochem. Cytochem.* 15:652–661.

Baroin, A., A. Bienvenue, and P. F. Devaux. 1979. Spin-label studies of protein-protein interactions in retinal rod outer segment membranes. Saturation transfer electron paramagnetic resonance spectroscopy. *Biochemistry.* 18:1151–1155.

Borggreven, J. M. P. M., F. J. M. Daemen, and S. L. Bonting. 1970. Biochemical aspects of the visual process. 6. Lipid composition of native and hexane-extracted cattle rod outer segments. *Biochim. Biophys. Acta.* 202:374–381.

Brown, P. K. 1972. Rhodopsin rotates in the visual receptor membrane. *Nat. New Biol.* 236:35–38.

Chambers, R. W., M. C. Bowling, and P. M. Grimley. 1968. Glutaraldehyde fixation in routine histopathology. *Arch. Pathol.* 85:18–30.

Cherry, R. J., A. Bürkli, M. Busslinger, G. Schneider, and G. R. Parish. 1976. Rotational diffusion of Band 3 proteins in the human erythrocyte membrane. *Nature (Lond.).* 263:389–393.

Cohen, A. I. 1972. Rods and cones. Handbook of Sensory Physiology. Part 2. M. G. F. Fuortes, editor. Springer-Verlag, Heidelberg. 7:72–73.

Cone, R. A. 1972. Rotational diffusion of rhodopsin in visual receptor membrane. *Nat. New Biol.* 236(63):39–43.

Converse, C. A. 1979. The large intrinsic membrane protein in rod outer segments: in vitro synthesis in cattle, and comparison in humans and rabbits. *Exp. Eye. Res.* 29:409–416.

Corless, J. M. 1980. The carbohydrates in frog retinal rod outer segments. *Prog Histochem. Cytochem.* 12:1–55.

Drzymala, R. E., H. L. Weiner, and P. A. Liebman. 1980. Limited lateral diffusion of porphyropsin in mudpuppy rod outer segment disks. *Fed. Proc.* 39:2137. (Abstr.)

Drzymala, R. E., P. A. Liebman, and Gy. Romhany. 1982. Acid polysaccharide content of frog rod outer segments determined by metachromatic toluidine blue staining. *Histochemistry.* 76:363–379.

Frasca, J., and V. Parks. 1965. A routine technique for double-staining ultrathin sections using uranyl and lead salts. *J. Cell Biol.* 25:157–161.

Frenkel, J. 1955. Orientation and rotational motion of molecules in liquid bodies. Surface and allied phenomena. *In* Kinetic Theory of Liquids. Dover Publications, Inc., New York. 250–353.

Goldsmith, T. H., and R. Wehner. 1977. Restrictions on rotational and translational diffusion of pigment in the membranes at a rhabdomeric photoreceptor. *J. Gen. Physiol.* 70:453–490.

Heller, J., T. Ostwald, and D. Bok. 1971. The osmotic behavior of rod photoreceptor outer segment disks. *J. Cell Biol.* 48:633–659.

Jost, W. 1952. Theory of diffusion in solids. *In* Diffusion in Solids, Liquids, Gases. Academic Press, Inc., New York. 135–178.

Korenstein, R., and B. Hess. 1978. Immobilization of bateriorhodopsin and orientation of its transition moment in purple membrane. *FEBS (Fed. Eur. Biochem. Soc.) Lett.* 89:15–20.

Liebman, P. A., and G. Entine. 1974. Lateral diffusion of visual pigment in photoreceptor disk membranes. *Sciences (Wash., DC).* 185:457–459.

Liebman, P. A., and E. N. Pugh, Jr. 1979. The control of phosphodiesterase in rod disk membranes: kinetics, possible mechanisms and significance for vision. *Vision Res.* 19:375–380.

Liebman, P. A., and E. N. Pugh, Jr. 1981. Control of rod disk membrane phosphodiesterase and a model for visual transduction. *Curr. Top. Membr. Trans.* 15:157–170.

Liebman, P. A., H. L. Weiner, and R. E. Drzymala. 1981. Lateral diffusion of pigment of visual cells. *Methods Enzymol.* 81:660–668.

Lux, S. E. 1979. Dissecting the red cell membrane skeleton. *Nature (Lond.).* 281:426–429.

Millonig, G. 1966. Model experiments on fixation and dehydration. *Proc. Sixth Int. Congr. Electron Microsc.* 2:21.

Nigg, E. A., and R. J. Cherry. 1980. Anchorage of a Band 3 population of the erythrocyte cytoplasmic membrane surface-protein rotational diffusion measurement. *Proc. Natl. Acad. Sci. USA.* 77:4702–4706.

Nir, I., and D. Pease. 1973. Ultrastructural aspects of disks in rod outer segments. *Exp. Eye Res.* 16:173–182.

Papermaster, D. S., B. G. Schneider, M. A. Zorn, and J. P. Kraehenbuhl. 1978. Immunocytochemical localization of a large intrinsic membrane protein to the incisure and margins of frog outer segment disks. *J. Cell Biol.* 78:415–425.

Poo, M., and R. A. Cone. 1974. Lateral diffusion of rhodopsin in the photoreceptor membrane. *Nature (Lond.).* 247:438–441.

Röhlich, P. 1976. Photoreceptor membrane carbohydrate on the intradical surface of retinal rod disks. *Nature (Lond.).* 263:789–791.

Steck, T. L. 1974. The organization of proteins in the human red blood cell membrane. *J. Cell Biol.* 62:1–19.

Spurr, A. 1969. A low-viscosity epoxy resin embedding medium for electron microscopy. *J. Ultrastruct. Res.* 26:31–43.

Takezoe, H., and H. Yu. 1981. Lateral diffusion of photopigments in photoreceptor disk membrane vesicles by the dynamic Kerr effect. *Biochemistry.* 20:5275–5281.

Tanford, C. 1961. Physical Chemistry of Macromolecules. John Wiley and Sons, Inc., New York. 317–363.

Tank, D. W., E. S. Wu, and W. W. Webb. 1981. Enhanced mobility of acetylcholine receptor and membrane probes in muscle membrane blebs. *Biophys. J.* 33(2, Pt. 2):74*a*. (Abstr.)

Trauble, H., and E. Sackmann. 1973. Lipid motion and rhodopin rotation. *Nature (Lond.).* 245:210–211.

Wey, C. L., and R. A. Cone. 1981. Lateral diffusion of rhodopsin in photoreceptor cells measured by fluorescence photobleaching and recovery. *Biophys. J.* 33:225–232.